

# Design, synthesis, and biological study of 4-[(2-nitroimidazole-1*H*-alkyloxy)aniline]-quinazolines as EGFR inhibitors exerting cytotoxicities both under normoxia and hypoxia

This article was published in the following Dove Press journal:  
*Drug Design, Development and Therapy*

Weiyang Cheng<sup>1,2,\*</sup>  
Suhua Wang<sup>1,2,\*</sup>  
Zhiheng Yang<sup>1,2</sup>  
Xin Tian<sup>1,2</sup>  
Yongzhou Hu<sup>3</sup>

<sup>1</sup>Department of Pharmacy, The First Affiliated Hospital of Zhengzhou University, Zhengzhou 450052, People's Republic of China; <sup>2</sup>Henan Key Laboratory of Precision Clinical Pharmacy, The First Affiliated Hospital of Zhengzhou University, Zhengzhou 450052, China; <sup>3</sup>Zhejiang Province Key Laboratory of Anti-Cancer Drug Research, College of Pharmaceutical Sciences, Zhejiang University, Hangzhou 310058, People's Republic of China

\*These authors contributed equally to this work

**Purpose:** In order to get novel EGFR inhibitors exerting more potency in tumor hypoxia than in normoxia.

**Methods:** A series of 4-[(2-nitroimidazole-1*H*-alkyloxy)aniline]-quinazolines were designed and synthesized, and their *in vitro* cytotoxicity and EGFR inhibitory activity were evaluated. Molecule docking study was performed for the representative compound.

**Results:** The structure-activity relationship (SAR) studies revealed that compounds bearing both meta-chloride and para-(2-nitroimidazole-1*H*-alkyloxy) groups on the aniline displayed potent inhibitory activities both in enzymatic and cellular levels. The most promising compound **16i** potently inhibited EGFR with an IC<sub>50</sub> value of 0.12 μM. Meanwhile, it manifested more potent cytotoxicity than the positive control lapatinib under tumor normoxia and hypoxia conditions (IC<sub>50</sub> values of 1.59 and 1.09 μM against A549 cells, 2.46 and 1.35 μM against HT-29 cells, respectively). The proposed binding model of **16i** in complex with EGFR was displayed by the docking results.

**Conclusion:** This study provides insights for developing hypoxia-activated kinase inhibitors.

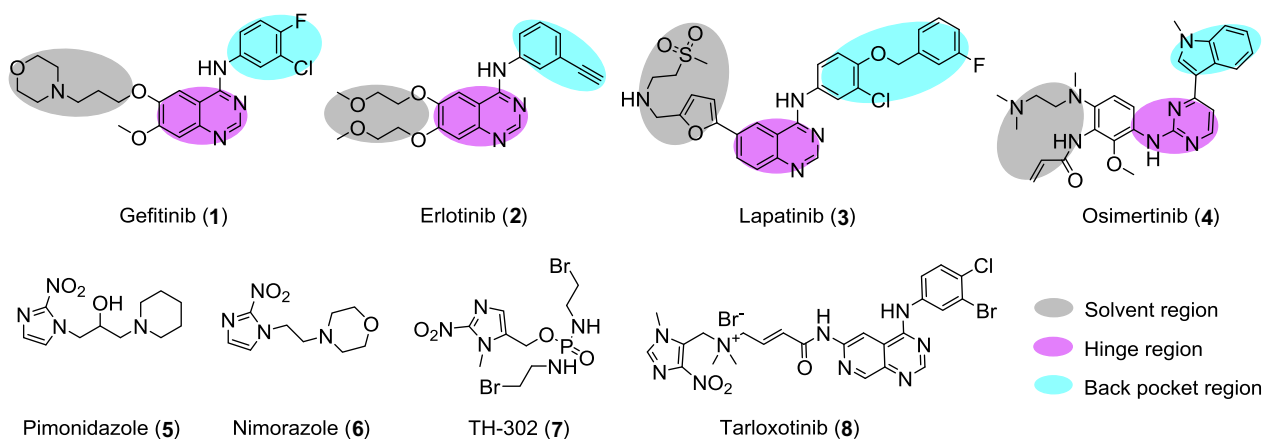
**Keywords:** EGFR inhibitor, hypoxia, tumor, 4-anilinoquinazoline, 2-nitroimidazole

## Introduction

EGFR is a trans-membrane protein that belongs to the HER family of receptor tyrosine kinases,<sup>1</sup> its overexpression has been confirmed in many solid carcinomas, which include non-small-cell lung carcinoma,<sup>2</sup> colon carcinoma,<sup>3</sup> ovarian carcinoma,<sup>4</sup> head and neck carcinoma,<sup>5</sup> and so on. On the other hand, hypoxia is unavoidable in solid carcinomas, it makes carcinomas resistant to radiotherapy and chemotherapy.<sup>6</sup> In particular, EGFR is massively overexpressed when carcinomas are under hypoxia.<sup>7,8</sup> The dual functions of EGFR overexpression and tumor hypoxia exhibit a great challenge to carcinoma treatment. In other words, if a drug can inhibit EGFR, and also be activated under carcinoma hypoxia, it may exert a stronger effect. Recently, many small molecule EGFR inhibitors have been successfully developed and introduced onto the market, these drugs include gefitinib (**1**),<sup>9</sup> erlotinib (**2**),<sup>10</sup> lapatinib (**3**),<sup>11</sup> osimertinib (**4**),<sup>12</sup> etc (Figure 1). In addition, reagents targeting carcinoma-hypoxia have been massively explored, including the 2-nitroimidazole derivative pimonidazole (**5**),<sup>13</sup> nimorazole (**6**),<sup>14</sup> and so on

Correspondence: Xin Tian  
Department of Pharmacy, The First Affiliated Hospital of Zhengzhou University, 1 Jianshedong Road, Zhengzhou 450052, People's Republic of China  
Email tianx@zzu.edu.cn

Yongzhou Hu  
Zhejiang Province Key Laboratory of Anti-Cancer Drug Research, College of Pharmaceutical Sciences, Zhejiang University, 388 Yuhangtang Road, Hangzhou 310058, People's Republic of China  
Email huyz@zju.edu.cn



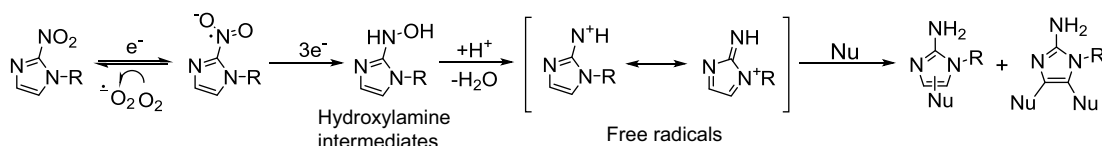
**Figure 1** Structures/depicted binding models of EGFR inhibitors (1–4, the depicted binding models of inhibitors with EGFR are shown in different colors), structures of 2-nitroimidazole derivatives (5 and 6) and clinically studied hypoxia-activated compounds (7 and 8).

(Figure 1). Moreover, compounds that have been combined with hypoxia-activated groups and other functional moieties have been widely reported.<sup>15,16,17</sup> For example, the hypoxia-activated prodrug TH-302 (7, Figure 1) is 270-fold more effective in carcinoma hypoxia than in normoxia;<sup>18</sup> the hypoxia-activated EGFR inhibitor tarloxotinib (8, Figure 1) has been advanced to a phase II clinical study due to its excellent potency.<sup>19</sup>

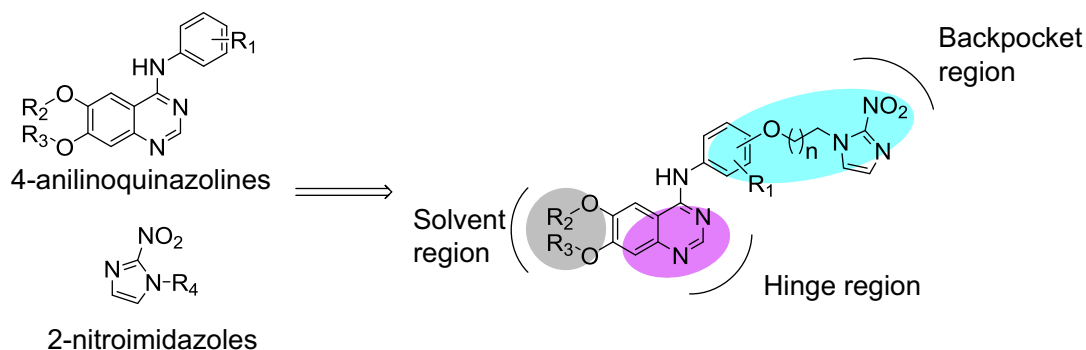
EGFR inhibitors compete with ATP to bind to kinase, blocking signal transduction and playing an inhibitory role.<sup>20</sup> Three main interaction regions, the solvent region, the hinge region, and the backpocket region, are involved in the inhibitor-EGFR kinase bindings (Figure 1).<sup>21</sup> In

carcinoma hypoxic environment, 2-nitroimidazole can be reduced to hydroxylamine intermediates through four-electron reduction. The intermediates are further reduced to free radicals under hypoxia, and covalently bind to nucleophilic proteins, amino acids, and other components to target tumors. In normoxia, the presence of oxygen prevents the 2-nitroimidazole group from being reduced and activated, and it exists in the prototype state, thus ensuring its safety in normal tissue (Figure 2).<sup>22</sup>

In order to get novel EGFR inhibitors that exert more potency in tumor hypoxia than in normoxia, we designed a series of compounds by combining 2-nitroimidazole group and 4-anilinoquinazolines (Figure 3). It has been



**Figure 2** Reductive activation mechanism of 2-nitroimidazole in carcinoma hypoxic environment.



**Figure 3** Our design strategy for EGFR inhibitors.

confirmed that the aniline group of 4-anilinoquinazoline was positioned in the backpocket region of EGFR kinase, and this space was enough to accommodate bulky moieties,<sup>23</sup> so we incorporated 2-nitroimidazole group into the aniline position herein (Figure 3). Meanwhile, different kinds of side chains at C-7 and C-8 of the quinazolines were chosen, referencing the structures of gefitinib and erlotinib. Through investigation of the aniline substituents and the styles of the side chain, the structure-activity relationships (SARs) of these compounds were studied.

## Methods and materials

### Chemistry

Melting points were determined by a B-540 Büchi melting-point apparatus, nuclear magnetic resonance (NMR) spectra were recorded on BRUKER AVIII 500 MHz or BRUKER AVII 400 MHz spectrometer (500 or 400 MHz for <sup>1</sup>H NMR, 100 MHz for <sup>13</sup>C NMR). Mass spectra were obtained on the Finnigan LCQ DecaXP ion trap mass spectrometer.

#### Procedure for the synthesis of substituted nitrobenzene (10a-d)

Dihalide alkane (30 mmol) was added to a stirred solution of substituted phenol (**9a-c**) (10 mmol) and K<sub>2</sub>CO<sub>3</sub> (5 mmol) in DMF (10 mL). The reaction mixture was heated to 60°C and stirred overnight. After the reaction was completed, the mixture was cooled to room temperature (rt) and filtered, the filtrate was removed in vacuo. Finally, silica gel column chromatography was used to purify the residue, and pure **10a-d** were obtained.

1-(2-Bromoethoxy)-2-chloro-4-nitrobenzene (**10a**): white solid. Yield: 64%, mp: 56°C–58°C. <sup>1</sup>H NMR (500 MHz, CDCl<sub>3</sub>) δ 8.33–8.30 (m, 1H), 8.16 (dd, *J* = 9.0, 2.5 Hz, 1H), 6.99 (d, *J* = 9.0 Hz, 1H), 4.45 (t, *J* = 6.5 Hz, 2H), 3.73 (t, *J* = 6.5 Hz, 2H). ESI-MS *m/z*: 280 [M+1]<sup>+</sup>.

1-(3-Bromopropoxy)-2-chloro-4-nitrobenzene (**10b**): white solid. Yield: 71%, mp: 52°C–54°C. <sup>1</sup>H NMR (500 MHz, CDCl<sub>3</sub>) δ 8.30 (d, *J* = 2.5 Hz, 1H), 8.17 (dd, *J* = 9.0, 2.5 Hz, 1H), 7.02 (d, *J* = 9.0 Hz, 1H), 4.30 (t, *J* = 5.5 Hz, 2H), 3.67 (t, *J* = 6.0 Hz, 2H), 2.46–2.39 (m, 2H). ESI-MS *m/z*: 296 [M+1]<sup>+</sup>.

1-(2-Chloroethoxy)-3-nitrobenzene (**10c**): white solid. Yield: 59%, mp: 57°C–59°C (lit. 59°C–60°C).<sup>24</sup>

1-(2-Bromoethoxy)-4-nitrobenzene (**10d**): white solid. Yield: 51%, mp: 59°C–61°C (lit. 62°C–64°C).<sup>25</sup>

#### Procedure for the synthesis of substituted aniline (11a-d)

To a solution of **10a-d** (10 mmol) in methanol (20 mL), and 10% Pd/C was added. Then **10a-d** were reduced by hydrogen at atmospheric pressure for about 2 hours and the catalyst was removed by filtration. The filtrate was evaporated to afford **11a-d** in the yields >93%.

4-(2-Bromoethoxy)-3-chloroaniline (**11a**): brown solid. Yield: 95%, mp: 68°C–70°C. <sup>1</sup>H NMR (500 MHz, CDCl<sub>3</sub>) δ 6.83 (d, *J* = 8.5 Hz, 1H), 6.73 (d, *J* = 3.0 Hz, 1H), 6.52 (dd, *J* = 8.5, 3.0 Hz, 1H), 4.24 (t, *J* = 6.5 Hz, 2H), 3.62 (t, *J* = 6.5 Hz, 2H), 3.53 (br, 2H). ESI-MS *m/z*: 252 [M+1]<sup>+</sup>.

4-(3-Bromopropoxy)-3-chloroaniline (**11b**): brown solid. Yield: 93%, mp: 62°C–64°C. <sup>1</sup>H NMR (500 MHz, CDCl<sub>3</sub>) δ 6.80 (d, *J* = 8.5 Hz, 1H), 6.74 (d, *J* = 3.0 Hz, 1H), 6.54 (dd, *J* = 8.5, 3.0 Hz, 1H), 4.07 (t, *J* = 5.5 Hz, 2H), 3.65 (t, *J* = 6.5 Hz, 2H), 3.25 (br, 2H), 2.34–2.28 (m, 2H). ESI-MS *m/z*: 266 [M+1]<sup>+</sup>.

3-(2-Chloroethoxy)-aniline (**11c**): colorless oil. Yield: 96%. <sup>1</sup>H NMR (500 MHz, CDCl<sub>3</sub>) δ 7.07 (t, *J* = 8.0 Hz, 1H), 6.38–6.32 (m, 2H), 6.30 (t, *J* = 2.5 Hz, 1H), 4.19 (t, *J* = 6.0 Hz, 2H), 3.79 (t, *J* = 6.0 Hz, 2H), 3.58 (br, 2H). ESI-MS *m/z*: 172 [M+1]<sup>+</sup>.

4-(2-Bromoethoxy)-aniline (**11d**): white solid. Yield: 100%, mp: 89°C–91°C. <sup>1</sup>H NMR (500 MHz, CDCl<sub>3</sub>) δ 6.79–6.75 (m, 2H), 6.67–6.61 (m, 2H), 4.21 (t, *J* = 6.5 Hz, 2H), 3.59 (t, *J* = 6.5 Hz, 2H), 3.44 (br, 2H). ESI-MS *m/z*: 216 [M+1]<sup>+</sup>.

#### Procedure for the synthesis of 2-nitroimidazole derivative (12a-d)

To a stirred solution of substituted aniline (**11a-d**) (10 mmol) and powdered K<sub>2</sub>CO<sub>3</sub> (5 mmol) in DMF (10 mL), 2-nitroimidazole (1.36g, 12 mmol) was added. The reaction mixture was heated to 70°C and stirred for about 10 hours. After the reaction was completed, the mixture was cooled to rt and filtered, the filtrate was removed in vacuo. Then methylene chloride was used to dissolve the obtained residue, which was further washed with water. Finally, the organic solvent was dried over sodium sulfate and concentrated to obtain crude **12a-d**, which were further purified by column chromatography to get pure materials.

3-Chloro-4-(2-(2-nitro-1H-imidazol-1-yl)ethoxy)aniline (**12a**): yellow solid. Yield: 55%, mp: 127°C–129°C. <sup>1</sup>H NMR (500 MHz, CDCl<sub>3</sub>) δ 7.38 (d, *J* = 1.0 Hz, 1H), 7.17 (d, *J* = 1.0 Hz, 1H), 6.70 (d, *J* = 3.0 Hz, 1H), 6.67 (d, *J* = 8.5

Hz, 1H), 6.50 (dd,  $J=8.5, 3.0$  Hz, 1H), 4.85–4.80 (m, 2H), 4.31–4.26 (m, 2H), 2.75 (br, 2H). ESI-MS  $m/z$ : 283  $[M+1]^+$ .

3-Chloro-4-(3-(2-nitro-1H-imidazol-1-yl)propoxy)aniline (**12b**): yellow solid. Yield: 53%, mp: 136°C–138°C.  $^1\text{H}$  NMR (500 MHz,  $\text{CDCl}_3$ )  $\delta$  7.17 (s, 1H), 7.11 (s, 1H), 6.76 (d,  $J=2.5$  Hz, 1H), 6.72 (d,  $J=8.5$  Hz, 1H), 6.53 (dd,  $J=8.5, 3.0$  Hz, 1H), 4.71 (t,  $J=6.5$  Hz, 2H), 3.89 (t,  $J=5.5$  Hz, 2H), 3.53 (br, 2H), 2.36–2.30 (m, 2H). ESI-MS  $m/z$ : 297  $[M+1]^+$ .

3-(2-(2-Nitro-1H-imidazol-1-yl)ethoxy)aniline (**12c**): brown solid. Yield: 58%, mp: 51°C–53°C.  $^1\text{H}$  NMR (500 MHz,  $\text{CDCl}_3$ )  $\delta$  7.23 (d,  $J=0.5$  Hz, 1H), 7.13 (d,  $J=1.0$  Hz, 1H), 7.02 (t,  $J=8.0$  Hz, 1H), 6.30 (dd,  $J=8.0, 2.0$  Hz, 1H), 6.22 (dd,  $J=8.0, 2.5$  Hz, 1H), 6.15 (t,  $J=2.0$  Hz, 1H), 4.77 (dd,  $J=12.5, 8.0$  Hz, 2H), 4.27 (dd,  $J=10.5, 5.5$  Hz, 2H), 4.04–3.10 (br, 2H). ESI-MS  $m/z$ : 249  $[M+1]^+$ .

4-(2-(2-Nitro-1H-imidazol-1-yl)ethoxy)aniline (**12d**): brown solid. Yield: 48%, mp: 48°C–50°C.  $^1\text{H}$  NMR (500 MHz,  $\text{CDCl}_3$ )  $\delta$  7.24 (d,  $J=1.0$  Hz, 1H), 7.14 (t,  $J=3.0$  Hz, 1H), 6.69–6.62 (m, 2H), 6.62–6.57 (m, 2H), 4.77 (dd,  $J=14.5, 10.0$  Hz, 2H), 4.25 (dd,  $J=13.5, 8.5$  Hz, 2H), 3.47 (br, 2H). ESI-MS  $m/z$ : 249  $[M+1]^+$ .

#### Procedure for the synthesis of 4-(3-((4-chloro-6-methoxyquinazolin-7-yl)oxy)propyl)morpholine (**13**)

Compound **13** was prepared following the published synthesis route.<sup>26</sup> Briefly, commercially available 6-methoxy-7-(3-morpholinopropoxy)quinazolin-4(3H)-one (2.0 g, 6.3 mmol) was mixed with  $\text{SOCl}_2$  (15 mL) and DMF (0.2 mL), then the mixture was heated at reflux temperature for 5 hours. The volatiles were removed under reduced pressure. The residue was dissolved in  $\text{CH}_2\text{Cl}_2$  (50 mL) and the organic layer was washed with aqueous  $\text{NaHCO}_3$  solution and brine, and dried over  $\text{Na}_2\text{SO}_4$ , filtered and evaporated to give the crude product **13**, which was purified by silica gel column chromatography to get pure intermediate **13** as a white solid. Yield: 48%, mp: 111°C–113°C.  $^1\text{H}$  NMR ( $\text{CDCl}_3$ , 500 MHz)  $\delta$  8.86 (s, 1H), 7.39 (s, 1H), 7.35 (s, 1H), 4.30 (t, 2H,  $J=6.4$  Hz), 4.05 (s, 3H), 3.85 (m, 4H), 2.33–2.94 (m, 6H), 2.20 (m, 2H). ESI-MS  $m/z$ : 338  $[M+1]^+$ .

#### Procedure for the synthesis of 4-chloro-6,7-bis(2-methoxyethoxy)quinazoline (**14**)<sup>27</sup>

Compound **14** was prepared in the same way as compound **13**, but the was changed from 6-methoxy-7-(3-morpholinopropoxy)quinazolin-4(3H)-one to 6,7-bis(2-methoxyethoxy)

quinazolin-4(3H)-one. White solid. Yield: 52%, mp: 105°C–107°C.  $^1\text{H}$  NMR (400 MHz,  $\text{CDCl}_3$ )  $\delta$  8.78 (s, 1H), 7.35 (s, 1H), 7.25 (s, 1H), 4.30–4.23 (m, 4H), 3.91–3.74 (m, 4H), 3.43 (s, 3H), 3.42 (s, 3H). ESI-MS  $m/z$ : 313  $[M+1]^+$ .

#### Procedure for the synthesis of 4-(3-((4-chloro-7-methoxyquinazolin-6-yl)oxy)propyl)morpholine (**15**)<sup>28</sup>

Compound **15** was prepared in the same way as compound **13**, but the start material was changed from 6-methoxy-7-(3-morpholinopropoxy)quinazolin-4(3H)-one to 7-methoxy-6-(3-morpholinopropoxy)quinazolin-4(3H)-one. White solid. Yield: 63%, mp: 119°C–121°C.  $^1\text{H}$  NMR (400 MHz,  $\text{CDCl}_3$ )  $\delta$  8.78 (s, 1H), 7.31 (s, 1H), 7.25 (s, 1H), 4.30–4.14 (m, 2H), 3.98 (s, 3H), 3.75–3.61 (m, 4H), 2.62–2.48 (m, 2H), 3.47–2.30 (m, 4H), 2.12–2.03 (m, 2H). ESI-MS  $m/z$ : 338  $[M+1]^+$ .

#### Procedure for the synthesis of the target compounds (**16a-l**)

To a stirred solution of 2-nitroimidazole derivative (**12a-d**) (1.0 mmol) in isopropyl alcohol (10 mL), compound **13**, **14** or **15** (1.0 mmol) was added. The mixture was reacted in reflux temperature and stirred for about 2 hours. After completion, the mixture was washed with saturated  $\text{NaHCO}_3$  solution and  $\text{CH}_2\text{Cl}_2$ , then the  $\text{CH}_2\text{Cl}_2$  solvent was dried by anhydrous  $\text{Na}_2\text{SO}_4$ , which was concentrated to obtain crude products **16a-l**. They were further purified by column chromatography to get pure materials.

N-(3-Chloro-4-(2-(2-nitro-1H-imidazol-1-yl)ethoxy)phenyl)-6-methoxy-7-(3-morpholinopropoxy)quinazolin-4-amine (**16a**): yellow solid. Yield: 83%, mp: 203°C–205°C.  $^1\text{H}$  NMR (500 MHz,  $\text{DMSO}-d_6$ )  $\delta$  9.41 (s, 1H), 8.42 (s, 1H), 7.91 (d,  $J=2.5$  Hz, 1H), 7.77 (s, 1H), 7.70 (s, 1H), 7.67 (dd,  $J=9.0, 2.5$  Hz, 1H), 7.20 (s, 1H), 7.16 (d,  $J=10.0$  Hz, 2H), 4.87 (t,  $J=5.0$  Hz, 2H), 4.43 (t,  $J=5.0$  Hz, 2H), 4.16 (t,  $J=6.5$  Hz, 2H), 3.93 (s, 3H), 3.61–3.54 (m, 4H), 2.47–2.30 (m, 6H), 1.98–1.91 (m, 2H).  $^{13}\text{C}$  NMR (100 MHz,  $\text{DMSO}-d_6$ )  $\delta$  156.6, 154.1, 153.3, 149.6, 149.5, 147.3, 145.4, 134.2, 128.8, 128.1, 124.2, 122.5, 121.2, 114.4, 109.1, 108.3, 102.4, 68.0, 67.2, 66.7 (2), 56.7, 55.2, 53.8 (2), 49.0, 26.1. ESI-MS  $m/z$ : 584  $[M+1]^+$ .

N-(3-Chloro-4-(3-(2-nitro-1H-imidazol-1-yl)propoxy)phenyl)-6-methoxy-7-(3-morpholinopropoxy)quinazolin-4-amine (**16b**): yellow solid. Yield: 81%, mp: 92°C–94°C.  $^1\text{H}$  NMR (500 MHz,  $\text{DMSO}-d_6$ )  $\delta$  9.42 (s, 1H), 8.43 (s, 1H), 7.92 (d,  $J=2.5$  Hz, 1H), 7.78 (s, 1H), 7.67 (dd,  $J=9.0, 2.5$  Hz, 1H), 7.65 (d,  $J=1.0$  Hz, 1H), 7.19–7.14 (m, 3H), 4.60 (t,  $J=7.0$  Hz, 2H), 4.16 (t,  $J=6.5$  Hz, 2H), 4.09 (t,  $J=6.0$  Hz, 2H), 3.94 (s, 3H), 3.57 (t,  $J=4.5$  Hz, 4H),

2.44 (t,  $J=7.0$  Hz, 2H), 2.40–2.34 (m, 4H), 2.33–2.26 (m, 2H), 2.00–1.89 (m, 2H).  $^{13}\text{C}$  NMR (100 MHz, DMSO- $d_6$ )  $\delta$  156.7, 154.1, 153.3, 150.1, 149.5, 147.4, 145.2, 134.0, 128.4, 128.2, 124.3, 122.6, 121.4, 114.5, 109.1, 108.4, 102.5, 67.2, 66.7 (2), 66.6, 56.7, 55.2, 53.8 (2), 47.3, 29.8, 26.1. ESI-MS  $m/z$ : 598  $[\text{M}+1]^+$ .

6-Methoxy-7-(3-morpholinopropoxy)-N-(3-(2-(2-nitro-1H-imidazol-1-yl)ethoxy)phenyl)quinazolin-4-amine (**16c**): yellow solid. Yield: 84%, mp: 149°C–151°C.  $^1\text{H}$  NMR (500 MHz, DMSO- $d_6$ )  $\delta$  9.38 (s, 1H), 8.44 (s, 1H), 7.80 (s, 1H), 7.71 (d,  $J=1.0$  Hz, 1H), 7.43 (dd,  $J=8.0$ , 1.5 Hz, 1H), 7.39 (t,  $J=2.0$  Hz, 1H), 7.26 (t,  $J=8.0$  Hz, 1H), 7.18 (d,  $J=1.0$  Hz, 1H), 7.16 (s, 1H), 6.65 (dd,  $J=8.0$ , 2.0 Hz, 1H), 4.82 (t,  $J=5.0$  Hz, 2H), 4.36 (t,  $J=5.0$  Hz, 2H), 4.17 (t,  $J=6.5$  Hz, 2H), 3.94 (s, 3H), 3.57 (t,  $J=4.5$  Hz, 4H), 2.44 (t,  $J=7.0$  Hz, 2H), 2.41–2.32 (m, 4H), 1.99–1.90 (m, 2H).  $^{13}\text{C}$  NMR (100 MHz, DMSO- $d_6$ )  $\delta$  158.4, 156.7, 154.1, 153.2, 149.5, 147.5, 145.4, 141.3, 129.7, 128.6, 128.1, 115.5, 109.4, 109.3, 109.2, 108.3, 102.5, 67.2, 66.7, 66.7 (2), 56.8, 55.2, 53.8 (2), 49.1, 26.1. ESI-MS  $m/z$ : 550  $[\text{M}+1]^+$ .

6-Methoxy-7-(3-morpholinopropoxy)-N-(4-(2-(2-nitro-1H-imidazol-1-yl)ethoxy)phenyl)quinazolin-4-amine (**16d**): yellow solid. Yield: 79%, mp: 152°C–154°C.  $^1\text{H}$  NMR (500 MHz, DMSO- $d_6$ )  $\delta$  9.36 (s, 1H), 8.35 (s, 1H), 7.79 (s, 1H), 7.71 (d,  $J=1.0$  Hz, 1H), 7.64–7.57 (m, 2H), 7.19 (d,  $J=1.0$  Hz, 1H), 7.13 (s, 1H), 6.94–6.87 (m, 2H), 4.81 (t,  $J=5.0$  Hz, 2H), 4.35 (t,  $J=5.0$  Hz, 2H), 4.15 (t,  $J=6.5$  Hz, 2H), 3.92 (s, 3H), 3.57 (t,  $J=4.0$  Hz, 4H), 2.46–2.41 (m, 2H), 2.41–2.33 (m, 4H), 2.01–1.85 (m, 2H).  $^{13}\text{C}$  NMR (100 MHz, DMSO- $d_6$ )  $\delta$  157.0, 154.6, 153.9, 153.5, 149.3, 147.2, 145.5, 133.4, 128.6, 128.1, 124.7 (2), 114.8 (2), 109.1, 108.3, 102.6, 67.2, 67.0, 66.7 (2), 56.7, 55.2, 53.8 (2), 49.1, 26.1. ESI-MS  $m/z$ : 550  $[\text{M}+1]^+$ .

N-(3-Chloro-4-(2-(2-nitro-1H-imidazol-1-yl)ethoxy)phenyl)-6,7-bis(2-methoxyethoxy)quinazolin-4-amine (**16e**): yellow solid. Yield: 84%, mp: 92°C–94°C.  $^1\text{H}$  NMR (500 MHz, DMSO- $d_6$ )  $\delta$  9.39 (s, 1H), 8.42 (s, 1H), 7.90 (s, 1H), 7.80 (s, 1H), 7.70 (s, 1H), 7.66 (dd,  $J=9.0$ , 2.0 Hz, 1H), 7.20–7.16 (m, 3H), 4.87 (t,  $J=4.5$  Hz, 2H), 4.43 (t,  $J=4.5$  Hz, 2H), 4.28–4.23 (m, 4H), 3.79–3.69 (m, 4H), 3.35 (s, 3H), 3.33 (s, 3H).  $^{13}\text{C}$  NMR (100 MHz, DMSO- $d_6$ )  $\delta$  156.7, 154.1, 153.3, 149.7, 148.6, 147.3, 145.4, 134.2, 128.8, 128.1, 124.2, 122.5, 121.3, 114.5, 109.2, 108.8, 103.8, 70.6, 70.6, 68.9, 68.5, 68.0, 58.9, 58.8, 49.0. ESI-MS  $m/z$ : 559  $[\text{M}+1]^+$ .

N-(3-Chloro-4-(3-(2-nitro-1H-imidazol-1-yl)propoxy)phenyl)-6,7-bis(2-methoxyethoxy)quinazolin-4-amine

(**16f**): yellow solid. Yield: 89%, mp: 90°C–92°C.  $^1\text{H}$  NMR (500 MHz, DMSO- $d_6$ )  $\delta$  9.41 (br, 1H), 8.43 (s, 1H), 7.91 (d,  $J=2.5$  Hz, 1H), 7.82 (s, 1H), 7.69–7.63 (m, 2H), 7.19 (s, 1H), 7.18 (d,  $J=1.0$  Hz, 1H), 7.16 (d,  $J=9.0$  Hz, 1H), 4.60 (t,  $J=7.0$  Hz, 2H), 4.26 (t,  $J=9.0$  Hz, 4H), 4.09 (t,  $J=6.0$  Hz, 2H), 3.76 (t,  $J=9.0$  Hz, 2H), 3.73 (t,  $J=9.0$  Hz, 2H), 3.35 (s, 3H), 3.33 (s, 3H).  $^{13}\text{C}$  NMR (100 MHz, DMSO- $d_6$ )  $\delta$  156.7, 154.1, 153.4, 150.2, 148.6, 147.3, 145.1, 133.9, 128.4, 128.2, 124.3, 122.6, 121.4, 114.5, 109.3, 108.8, 103.9, 70.6, 70.5, 68.9, 68.5, 66.6, 58.9, 58.8, 47.3, 29.8. ESI-MS  $m/z$ : 573  $[\text{M}+1]^+$ .

6,7-Bis(2-methoxyethoxy)-N-(3-(2-(2-nitro-1H-imidazol-1-yl)ethoxy)phenyl)quinazolin-4-amine (**16g**): yellow solid. Yield: 81%, mp: 183°C–185°C.  $^1\text{H}$  NMR (400 MHz, DMSO- $d_6$ )  $\delta$  9.39 (s, 1H), 8.46 (s, 1H), 7.86 (s, 1H), 7.73 (d,  $J=1.2$  Hz, 1H), 7.44 (dd,  $J=8.0$ , 1.2 Hz, 1H), 7.41 (t,  $J=2.0$  Hz, 1H), 7.27 (t,  $J=8.0$  Hz, 1H), 7.22 (s, 1H), 7.20 (d,  $J=1.2$  Hz, 1H), 6.66 (dd,  $J=8.0$ , 2.0 Hz, 1H), 4.84 (t,  $J=5.2$  Hz, 2H), 4.38 (t,  $J=5.2$  Hz, 2H), 4.32–4.24 (m, 4H), 3.81–3.72 (m, 4H), 3.37 (s, 3H), 3.35 (s, 3H).  $^{13}\text{C}$  NMR (100 MHz, CDCl $_3$ )  $\delta$  158.2, 156.3, 154.7, 153.3, 149.0, 147.1, 140.1, 129.9 (2), 128.3, 127.2, 114.8, 110.0, 109.1, 108.5, 108.1, 102.7, 71.0, 70.5, 69.3, 68.4, 66.2, 59.3, 59.3, 49.4. ESI-MS  $m/z$ : 525  $[\text{M}+1]^+$ .

6,7-Bis(2-methoxyethoxy)-N-(4-(2-(2-nitro-1H-imidazol-1-yl)ethoxy)phenyl)quinazolin-4-amine (**16h**): white solid. Yield: 83%, mp: 196°C–198°C.  $^1\text{H}$  NMR (500 MHz, DMSO- $d_6$ )  $\delta$  9.34 (s, 1H), 8.35 (s, 1H), 7.82 (s, 1H), 7.71 (d,  $J=1.0$  Hz, 1H), 7.62–7.58 (m, 2H), 7.19 (d,  $J=1.0$  Hz, 1H), 7.16 (s, 1H), 6.94–6.88 (m, 2H), 4.81 (t,  $J=5.0$  Hz, 2H), 4.35 (t,  $J=5.0$  Hz, 2H), 4.29–4.21 (m, 4H), 3.78–3.74 (m, 2H), 3.74–3.69 (m, 2H), 3.35 (s, 3H), 3.33 (s, 3H).  $^{13}\text{C}$  NMR (100 MHz, DMSO- $d_6$ )  $\delta$  157.0, 154.6, 154.0, 153.5, 148.4, 147.2, 145.5, 133.3, 128.6, 128.1, 124.7 (2), 114.8 (2), 109.2, 108.7, 104.0, 70.6, 70.6, 68.9, 68.5, 67.0, 58.9, 58.8, 49.1. ESI-MS  $m/z$ : 525  $[\text{M}+1]^+$ .

N-(3-Chloro-4-(2-(2-nitro-1H-imidazol-1-yl)ethoxy)phenyl)-7-methoxy-6-(3-morpholinopropoxy)quinazolin-4-amine (**16i**): yellow solid. Yield: 65%, mp: 132°C–134°C.  $^1\text{H}$  NMR (500 MHz, DMSO- $d_6$ )  $\delta$  9.56 (s, 1H), 8.46 (s, 1H), 7.96 (d,  $J=2.5$  Hz, 1H), 7.91 (s, 1H), 7.77–7.69 (m, 2H), 7.27–7.13 (m, 3H), 4.90 (t,  $J=5.0$  Hz, 2H), 4.45 (t,  $J=5.0$  Hz, 2H), 4.23 (t,  $J=5.5$  Hz, 2H), 3.94 (s, 3H), 3.88–3.60 (m, 4H), 3.44–3.22 (m, 6H), 2.24–2.04 (m, 2H).  $^{13}\text{C}$  NMR (100 MHz, DMSO- $d_6$ )  $\delta$  156.8, 154.9, 153.2, 149.7, 148.4, 147.0, 145.4, 134.2, 128.8, 128.1, 124.3, 122.6,

121.2, 114.4, 109.2, 107.6, 104.0, 68.0, 67.4, 64.7, 56.4 (2), 54.6, 52.3, 49.0 (2), 24.4. ESI-MS *m/z*: 584 [M+1]<sup>+</sup>.

N-(3-Chloro-4-(3-(2-nitro-1H-imidazol-1-yl)propoxy)phenyl)-7-methoxy-6-(3-morpholinopropoxy)quinazolin-4-amine (**16j**): yellow solid. Yield: 59%, mp: 107°C–109°C. <sup>1</sup>H NMR (500 MHz, CDCl<sub>3</sub>) δ 8.63 (s, 1H), 7.90 (d, *J*=2.5 Hz, 1H), 7.70 (br, 1H), 7.57 (dd, *J*=9.0, 2.5 Hz, 1H), 7.35 (s, 1H), 7.25 (s, 1H), 7.18 (s, 1H), 7.13 (d, *J*=0.5 Hz, 1H), 6.91 (d, *J*=9.0 Hz, 1H), 4.74 (t, *J*=6.5 Hz, 2H), 4.26 (t, *J*=6.5 Hz, 2H), 4.04–3.96 (m, 5H), 3.83 (t, *J*=4.5 Hz, 4H), 2.74 (t, *J*=7.0 Hz, 2H), 2.70–2.61 (m, 4H), 2.44–2.36 (m, 2H), 2.24–2.16 (m, 2H). <sup>13</sup>C NMR (100 MHz, DMSO-*d*<sub>6</sub>) δ 156.7, 154.9, 153.3, 150.2, 148.7, 147.3, 145.4, 133.9, 128.4, 128.2, 124.4, 122.7, 121.4, 114.4, 109.2, 107.8, 103.2, 67.6, 66.6 (2), 66.5, 56.3, 55.4, 53.9 (2), 47.3, 29.8, 26.3. ESI-MS *m/z*: 598 [M+1]<sup>+</sup>.

7-Methoxy-6-(3-morpholinopropoxy)-N-(3-(2-(2-nitro-1H-imidazol-1-yl)ethoxy)phenyl)quinazolin-4-amine (**16k**): yellow solid. Yield: 58%, mp: 60°C–62°C. <sup>1</sup>H NMR (400 MHz, CDCl<sub>3</sub>): 8.61 (s, 1H, CH), 7.82 (br, 1H), 7.49 (t, *J*=2.0 Hz, 1H), 7.35–7.27 (m, 4H), 7.25 (s, 1H), 7.15 (d, *J*=1.2 Hz, 1H), 4.84 (t, *J*=9.6 Hz, 2H), 4.39 (t, *J*=9.6 Hz, 2H), 4.24 (t, *J*=6.8 Hz, 2H), 3.99 (s, 3H), 3.79 (t, *J*=9.2 Hz, 4H), 2.69 (t, *J*=7.2 Hz, 2H), 2.62 (t, *J*=9.2 Hz, 4H), 2.17–2.15 (m, 2H). <sup>13</sup>C NMR (100 MHz, DMSO-*d*<sub>6</sub>) δ 158.4, 156.7, 154.9, 153.2, 148.7, 147.5, 145.5, 141.2, 129.7, 128.6, 128.1, 115.6, 109.4 (2), 109.3, 107.8, 103.3, 67.7, 66.7, 66.6 (2), 56.3, 55.4, 53.9 (2), 49.1, 26.3. ESI-MS *m/z*: 550 [M+1]<sup>+</sup>.

7-Methoxy-6-(3-morpholinopropoxy)-N-(4-(2-(2-nitro-1H-imidazol-1-yl)ethoxy)phenyl)quinazolin-4-amine (**16l**): yellow solid. Yield: 55%, mp: 212°C–214°C. <sup>1</sup>H NMR (400 MHz, CDCl<sub>3</sub>) δ 8.58 (s, 1H), 7.61–7.56 (m, 2H), 7.40 (s, 1H), 7.27 (d, *J*=1.2 Hz, 2H), 7.24 (s, 1H), 7.22 (s, 1H), 7.17 (d, *J*=1.2 Hz, 1H), 6.93–6.84 (m, 2H), 4.87–4.82 (m, 2H), 4.44–4.31 (m, 2H), 4.23 (t, *J*=6.8 Hz, 2H), 4.00 (s, 3H), 3.79–3.75 (m, 4H), 2.65 (t, *J*=5.6 Hz, 2H), 2.60–2.54 (m, 4H), 2.19–2.10 (m, 2H). <sup>13</sup>C NMR (100 MHz, DMSO-*d*<sub>6</sub>) δ 156.6, 154.3, 154.2, 153.0, 148.1, 146.8, 145.0, 132.9, 128.2, 127.7, 124.4 (2), 114.37 (2), 108.8, 107.3, 102.8, 67.2, 66.5, 66.2 (2), 55.8, 55.0, 53.5 (2), 48.7, 25.9. ESI-MS *m/z*: 550 [M+1]<sup>+</sup>.

### In vitro enzymatic activity assay

Activity of kinases was determined using Z'-Lyte Kinase Kit (Thermo Fisher Scientific, Waltham, MA, USA) according to the instructions.<sup>29</sup> The compounds were first tested the inhibition percentage at the concentration of 1.0×10<sup>-6</sup> mol/L. If the inhibition percentage was higher than 50%, these compounds were further chosen to test

their IC<sub>50</sub> values. For the IC<sub>50</sub> values, ten concentration gradients from 5.1×10<sup>-11</sup> to 1.0×10<sup>-6</sup> mol/L were set for the tested compounds. The experiments were performed according to the instructions of the manufacturer.

### Cytotoxicity assay

The cytotoxicity assay was performed as described previously.<sup>16,17</sup> Two human cancer cell lines (A549 and HT-29) were purchased from Cell Bank of China Science Academy (Shanghai, People's Republic of China). The cells were cultured in RPMI-1640 (Thermo Fisher Scientific) medium with heat-inactivated 10% FBS, penicillin (100 units/mL), and streptomycin (100 mg/mL) and incubated at 37°C. The cytotoxic activity in vitro was measured using sulforhodamine B (SRB) assay. All the compounds were dissolved in DMSO at the concentration 10.0 mg/mL and were then diluted to the appropriate concentrations. Cells were plated in 96-well plates (5×10<sup>3</sup> per well) for 24 hours and subsequently treated with different concentrations of all tested compounds under normoxia or hypoxia for 72 hours, respectively. Cells were then washed with PBS and fixed with 10% (w/v) trichloroacetic acid at 4°C for 1 hour. After washing, the cells were stained for 30 minutes with 0.4% SRB dissolved in 1% acetic acid. Then the cells were washed with 1% acetic acid five times, and protein-bound dye was extracted with 10 mmol unbuffered Tris base. The absorbance was measured at 515 nm using a multiscan spectrum (Thermo Electron Co., Vantaa, Finland). The inhibition rate on cell proliferation of each well was calculated as (A515 control cells - A515 treated cells)/A515 control cells ×100%, and the IC<sub>50</sub> values were determined by Logit method.

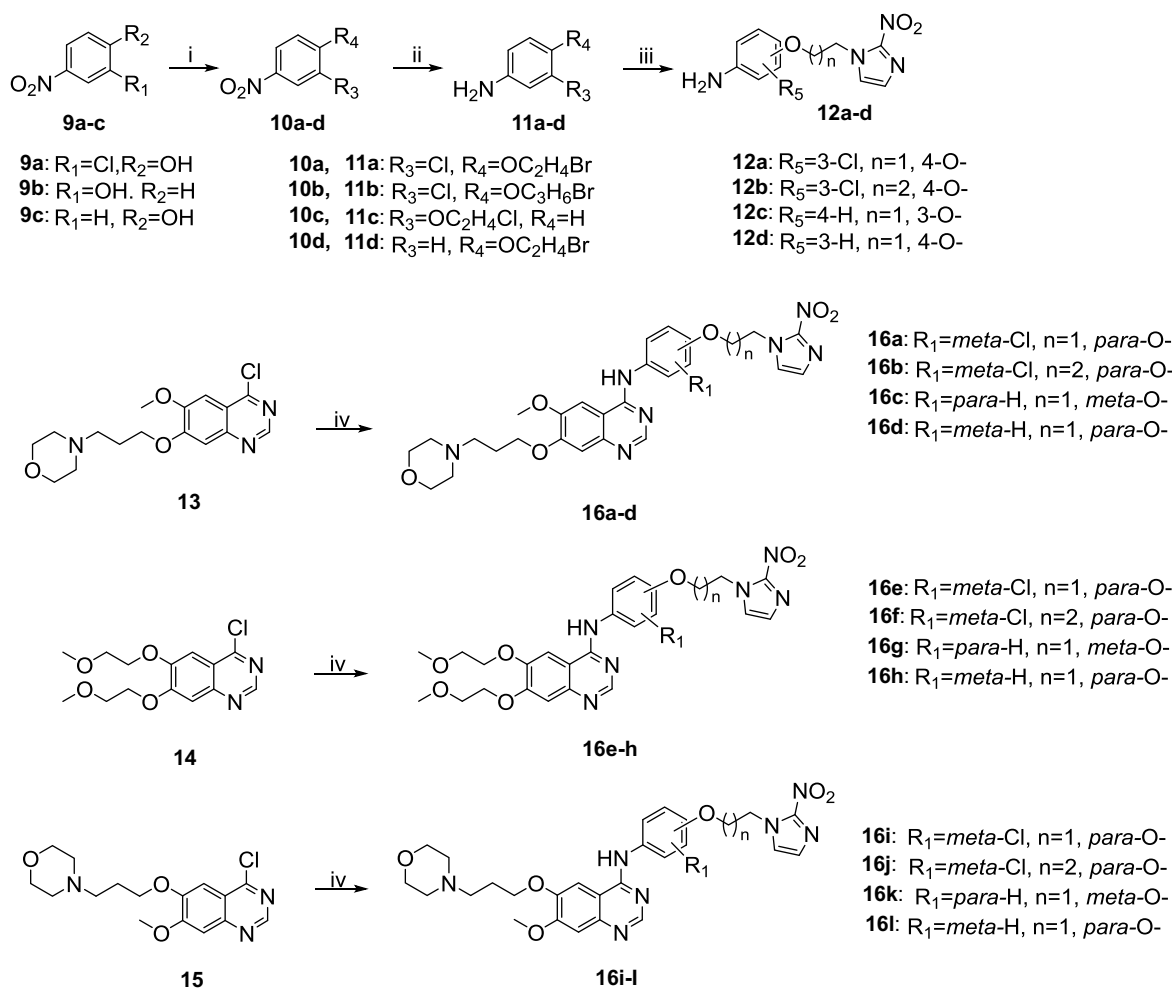
### Molecular modeling

According to the docking mode of compound **16i** with EGFR, the co-crystal structure of EGFR/lapatinib was chosen as the template (PDB ID: 1XKK). The docking procedure was carried out by using C-DOCKER protocol within Discovery Studio 2.1. The detailed process has been described previously, and the pictures were prepared using Pymol.<sup>16,17</sup>

## Results and discussion

### Synthesis

Synthesis of the target compounds **16a-l** followed the general pathway shown in Scheme 1. The start materials **9a-c** reacted with α, ω-dihalide alkane in the presence of potassium carbonate to afford **10a-d**, then they were



**Scheme 1** Reagents and conditions: i)  $\alpha, \omega$ -dihalide alkane,  $\text{K}_2\text{CO}_3$ , DMF,  $60^\circ\text{C}$ , overnight; ii)  $\text{H}_2$ , Pd/C, MeOH, room temperature, 2 hours; iii) 2-nitroimidazole,  $\text{K}_2\text{CO}_3$ , DMF,  $70^\circ\text{C}$ , 10 hours; iv) **12a-d**, isopropanol, reflux, 2 hours.

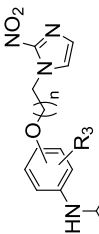
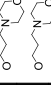



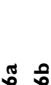
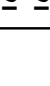
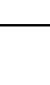

reduced with hydrogen to generate **11a-d**. Coupling **11a-d** with 2-nitroimidazole in the presence of potassium carbonate to obtain intermediates **12a-d**. In addition, compounds **13**, **14**, and **15** were prepared following the published synthesis route.<sup>26,27,28</sup> Finally, condensing **12a-d** with **13** in isopropanol to furnish the target compounds **16a-l**. Compounds **16e-h** and **16i-l** were obtained in a similar way by condensing **12a-d** with compound **14** and **15**, respectively.

## Enzymatic activity

The inhibitory activity of compound **16a-l** against EGFR was summarized in Table 1. Half of the tested compounds (**16a**, **16b**, **16e**, **16f**, **16i**, and **16j**) manifested potent activities, with the  $\text{IC}_{50}$  values ranging from 0.12–0.40  $\mu\text{M}$ . As expected, the meta-chloride substituent on aniline was crucial to the EGFR inhibitory activity. For example, compounds **16d**, **16h**, and **16l**, bearing no chloride group on

the aniline, only exhibited the inhibited rate lower than 50% at 1.0  $\mu\text{M}$ . While meta-chloride-bearing compounds **16a**, **16e**, and **16i** displayed the  $\text{IC}_{50}$  values of 0.19, 0.23, and 0.12  $\mu\text{M}$ , respectively. The bindings of lapatinib/EGFR indicate that the chloride atom of lapatinib takes up a small cavity comprised by Leu788, Thr790, and Ala743,<sup>23</sup> it seems that the chloride atom of this series exerts similar effects. The position of linker impacts activities as well, compounds with 2-nitroimidazole-1*H*-alkoxy moieties at the meta-position exhibited decreased enzymatic inhibitory activities compared to those at para-positions (**16c** vs **16d**, **16g** vs **16h**, and **16k** vs **16l**, inhibition% at 1.0  $\mu\text{M}$ : 24% vs 42%, 28% vs 44%, and 30% vs 45%, respectively). The length of the alkyloxy linker between aniline and 2-nitroimidazole also had obvious impact on the enzymatic inhibitory activities. The compromised EGFR inhibitory activities of compounds **16b**, **16f**, and **16j** ( $\text{IC}_{50}$ : 0.33, 0.40, and 0.18  $\mu\text{M}$ , respectively) compared with **16a**, **16e**,

Table 1 EGFR inhibitory activity and cytotoxicity of compounds **16a-l**

Compound	R <sub>1</sub>	R <sub>2</sub>	R <sub>3</sub>	n		EGFR IC <sub>50</sub> (μM)/inhibition% <sup>a</sup>	A549 (IC <sub>50</sub> , μM)		HT-29 (IC <sub>50</sub> , μM)	
							N <sup>b</sup>	H <sup>c</sup>	N	H
<b>16a</b>	OCH <sub>3</sub>		3-Cl	1	para-	0.19±0.04	3.88±0.81	2.62±1.06	3.97±2.06	2.33±0.40
<b>16b</b>	OCH <sub>3</sub>		3-Cl	2	para-	0.33±0.07	7.35±0.75	4.79±1.76	6.23±2.91	3.14±0.42
<b>16c</b>	OCH <sub>3</sub>		-	1	meta-	24	>50	>50	>50	>50
<b>16d</b>	OCH <sub>3</sub>		-	1	para-	42	29.47±8.41	18.48±5.15	19.37±6.70	14.32±2.38
<b>16e</b>			3-Cl	1	para-	0.23±0.03	5.42±1.33	2.68±1.38	4.54±2.03	2.36±0.55
<b>16f</b>			3-Cl	2	para-	0.40±0.06	15.79±3.49	10.28±3.97	9.26±2.90	6.20±1.48
<b>16g</b>			-	1	meta-	28	>50	>50	>50	19.84±4.16
<b>16h</b>			-	1	para-	44	5.42±2.07	2.68±1.52	4.54±1.69	2.36±1.21
<b>16i</b>		OCH <sub>3</sub>	3-Cl	1	para-	0.12±0.02	1.59±0.81	1.09±0.88	2.46±1.56	1.35±0.91
<b>16j</b>		OCH <sub>3</sub>	3-Cl	2	para-	0.18±0.04	6.51±1.83	4.35±1.82	5.96±2.44	3.63±1.61
<b>16k</b>		OCH <sub>3</sub>	-	1	meta-	30	47.39±6.17	30.14±6.18	>50	>50
<b>16l</b>		OCH <sub>3</sub>	-	1	para-	45	7.13±1.87	5.67±2.89	6.11±2.18	3.15±0.76
Lapatinib	-	-	-	-	-	0.011±0.003	11.30±2.34	13.26±3.66	6.81±1.24	8.85±1.05
Tirapazamine	-	-	-	-	-	-	>50	5.90±2.00	>50	8.45±1.85

Notes: <sup>a</sup>The EGFR inhibitory activities for **16c**, **16d**, **16g**, **16h**, **16k**, and **16l** were indicated as inhibition percentage (1.0 μM) and for others as IC<sub>50</sub> values (μM). <sup>b</sup>N, normoxia; <sup>c</sup>H, hypoxia.



and **16i** ( $IC_{50}$ : 0.19, 0.23, and 0.12  $\mu$ M, respectively) indicated that shorter linkers ( $n=1$ ) were more favorable than longer ones ( $n=2$ ), probably because longer linkers restricted the molecules from adapting the kinase. Moreover, the types and positions of groups adjusting physicochemical properties affected activities as well. Compounds with 6-morpholinopropoxyl-7-methoxy side chains (**16i-l**) exhibited more potent EGFR inhibitory activities than those with 6, 7-dimethoxyethoxy (**16e-h**) or 6-methoxyl-7-morpholinopropoxy (**16a-d**) ones.

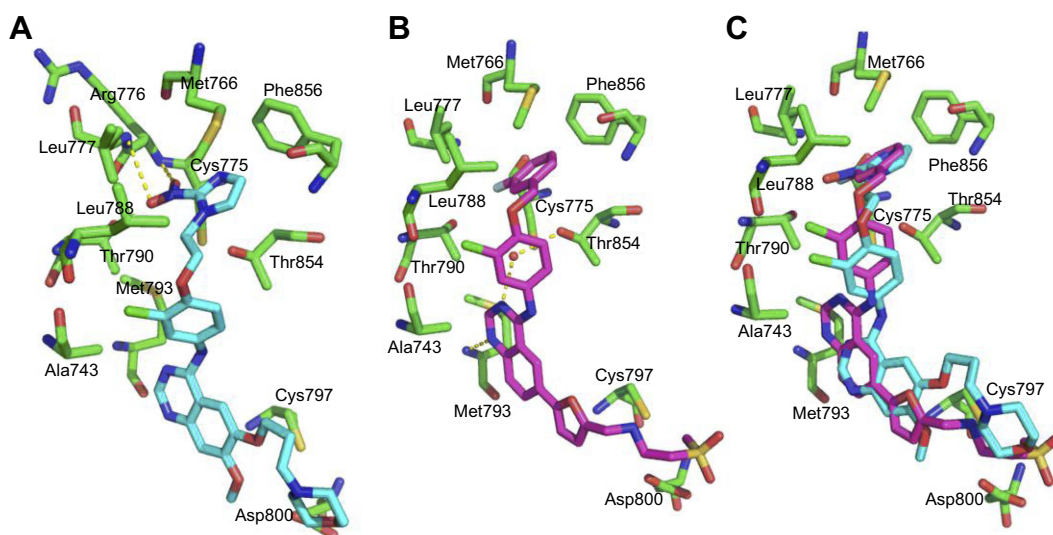
### In vitro cytotoxicity

The in vitro cytotoxicities of compounds **16a-l** were evaluated on human non-small-cell lung cancer A549 cells and human colorectal adenocarcinoma HT-29 cells under normoxic and hypoxic conditions (Table 1). Seven of all the 12 new compounds (**16a**, **16b**, **16e**, **16f**, **16i**, **16j**, and **16l**) exhibited good anti-proliferation activities. The SARs analysis indicated that both the introduction of 2-nitroimidazole-*IH*-alkoxy moieties at the aniline- para-position and the 3'-chloro substitution were favorable in terms of cytotoxicity (**16a** > **16c**, **16e** > **16g**, and **16i** > **16k**), and the results were consistent with the enzymatic inhibitory activities. Almost all of these compounds manifested comparable to more potent cytotoxicities against A549 and HT-29 cells under normoxia compared to under hypoxia. Although the difference in cytotoxicity was not obvious between hypoxia and normoxia, considering EGFR expression was significantly up-regulated under hypoxia,

which could partly offset the cytotoxicity generated in that circumstance,<sup>17</sup> it was speculated that the 2-nitroimidazole moieties underwent a bio-reductive activated process and exerted cytotoxicity especially under tumor hypoxia. Particularly, the most potent compound, **16i**, exhibited corresponding  $IC_{50}$  values of 1.59 and 1.09  $\mu$ M under normoxia and hypoxia against A549 cells, 2.46 and 1.35  $\mu$ M under normoxia and hypoxia against HT-29 cells, which were superior to the positive control lapatinib.

### Molecular docking study

The possible binding modes of these compounds in complex with EGFR were explored through a molecular modeling study between **16i** and the reported EGFR crystal structure (PDB ID: 1XKK). As illustrated in Figure 4, compound **16i** bound in the ATP-binding pocket of EGFR, which is similar to that of lapatinib. The 2-nitroimidazole group of **16i** was surrounded by the residues of Thr854, Phe856, Met766, and Leu777. Two hydrogen bonds were formed between the two oxygen atoms of 2-nitroimidazole and the residues of Arg776 and Leu777 of EGFR. In addition, the 3'-chloro group of the aniline was inserted in a pocket formed by the residues of Ala743, Thr790, and Leu788 (Figure 4A). Although compounds with two carbon linkers between aniline and 2-nitroimidazole moiety exhibited good EGFR inhibitory activity, this linker still appeared crowded and repulsed the 4-anilinoquinazoline group to the more "out" position than lapatinib (Figure 4C). This caused the quinazoline group to not form



**Figure 4** (A) Proposed binding models of compound **16i** in complex with EGFR. (B) Co-crystal structures of lapatinib in complex with EGFR (PDB code: 1XKK). (C) Comparison of the bindings of compound **16i** (purplish red) and lapatinib (cyan).

hydrogen bonds with Thr790 or Thr854, which was observed in lapatinib-EGFR complex (Figure 4B). We speculate that the loss of these important interactions led compound **16i** to display weaker EGFR inhibitory activity than lapatinib ( $IC_{50}$ : 0.12  $\mu$ M vs 0.011  $\mu$ M, Table 1). These results provide guidance for the further optimization of this series of compounds.

## Conclusion

For the purpose of getting novel EGFR inhibitors and taking advantage of the carcinoma hypoxia circumstance, a series of small molecule inhibitors was designed and synthesized by incorporating 2-nitroimidazole group into the aniline of the 4-anilinoquinazolines. The SARs studies revealed that the introduction of chloride at the meta-position and the 2-nitroimidazole-1*H*-alkoxy moiety at para-position of the aniline were crucial to the EGFR inhibitory activity. Meanwhile, the optimal alkyl linker between aniline and 2-nitroimidazole moiety was two carbons in these compounds. The anti-proliferative activities were consistent with the EGFR inhibitory activities, and almost all the new compounds exhibited more potent cytotoxicities under hypoxia than normoxia. In particular, the most promising compound, **16i**, exhibited good EGFR inhibitory activity ( $IC_{50}$  value of 0.12  $\mu$ M) and more potent cytotoxicities (A549 cells:  $IC_{50}$  values of 1.59 and 1.09  $\mu$ M under normoxia and hypoxia, respectively; HT-29 cells:  $IC_{50}$  values of 2.46 and 1.35  $\mu$ M under normoxia and hypoxia, respectively) than lapatinib. Moreover, the docking study confirmed the binding models between **16i** and EGFR. These results provide new insights for development of EGFR inhibitors exerting activities both under normoxia and hypoxia.

## Acknowledgments

The authors are grateful for the support of the National Natural Science Foundation of China (81703417), the Major Science and Technology Project of Henan Province (161100310100), and Henan Medical Science and Technology Research Project (2018020039). Dr Weiyan Cheng is grateful for the support of the Young Scholar Fund from The First Affiliated Hospital of Zhengzhou University.

## Disclosure

The authors report no conflicts of interest in this work.

## References

- Chong CR, Janne PA. The quest to overcome resistance to EGFR-targeted therapies in cancer. *Nat Med.* 2013;19(11):1389–1400. doi:10.1038/nm.3388
- Oronsky B, Ma P, Reid TR, et al. Navigating the “no man’s land” of TKI-failed EGFR-mutated non-small cell lung cancer (NSCLC): a review. *Neoplasia.* 2018;20(1):92–98. doi:10.1016/j.neo.2017.11.001
- Stintzing S, Tejpar S, Gibbs P, et al. Understanding the role of primary tumour localisation in colorectal cancer treatment and outcomes. *Eur J Cancer.* 2017;84:69–80. doi:10.1016/j.ejca.2017.07.016
- Cortez AJ, Tudrej P, Kujawa KA, et al. Advances in ovarian cancer therapy. *Cancer Chemoth Pharm.* 2018;81(1):17–38. doi:10.1007/s00280-017-3501-8
- Matsumoto Y, Sakurai H, Kogashiwa Y, et al. Inhibition of epithelial-mesenchymal transition by cetuximab via the EGFR-GEP100-Arf6-AMAP1 pathway in head and neck cancer. *Head Neck.* 2017;39(3):476–485. doi:10.1002/hed.24626
- Wilson WR, Hay MP. Targeting hypoxia in cancer therapy. *Nat Rev Cancer.* 2011;11(6):393–410. doi:10.1038/nrc3064
- Wang T, Niki T, Goto A, et al. Hypoxia increases the motility of lung adenocarcinoma cell line A549 via activation of the epidermal growth factor receptor pathway. *Cancer Sci.* 2007;98(4):506–511. doi:10.1111/j.1349-7006.2007.00428.x
- Nishi H, Nishi KH, Johnson AC. Early growth response-1 gene mediates up-regulation of epidermal growth factor receptor expression during hypoxia. *Cancer Res.* 2002;62(3):827–834.
- Rawluk J, Waller CF. Gefitinib. *Recent Results Cancer Res.* 2018;211:235–246. doi:10.1007/978-3-319-91442-8\_16
- Lyseng-Williamson KA. Erlotinib: a pharmaco-economic review of its use in advanced non-small cell lung cancer. *Pharmacoeconomics.* 2010;28(1):75–92. doi:10.2165/10482880-000000000-00000
- Medina PJ, Goodin S. Lapatinib: a dual inhibitor of human epidermal growth factor receptor tyrosine kinases. *Clin Ther.* 2008;30(8):1426–1447. doi:10.1016/j.clinthera.2008.08.008
- Greig SL. Osimertinib: first global approval. *Drugs.* 2016;76(2):263–273. doi:10.1007/s40265-015-0533-4
- Wack LJ, Monnich D, Yaromina A, et al. Correlation of FMISO simulations with pimonidazole-stained tumor xenografts: a question of  $O_2$  consumption? *Med Physics.* 2016;43(7):4113. doi:10.1118/1.4951728
- Hassan Metwally MA, Jansen JA, Overgaard J. Study of the population pharmacokinetic characteristics of nimorazole in head and neck cancer patients treated in the DAHANCA-5 trial. *Clin Oncol.* 2015;27(3):168–175. doi:10.1016/j.clon.2014.11.024
- Wei H, Li D, Yang X, et al. Design and synthesis of vandetanib derivatives containing nitroimidazole groups as tyrosine kinase inhibitors in normoxia and hypoxia. *Molecules.* 2016;21:12. doi:10.3390/molecules21121693
- Cheng W, Yuan Y, Qiu N, et al. Identification of novel 4-anilinoquinazoline derivatives as potent EGFR inhibitors both under normoxia and hypoxia. *Bioorg Med Chem.* 2014;22(24):6796–6805. doi:10.1016/j.bmc.2014.10.038
- Cheng W, Zhu S, Ma X, et al. Design, synthesis and biological evaluation of 6-(nitroimidazole-1*H*-alkyloxy)-4-anilinoquinazolines as efficient EGFR inhibitors exerting cytotoxic effects both under normoxia and hypoxia. *Eur J Med Chem.* 2015;89:826–834. doi:10.1016/j.ejmech.2014.11.010
- Duan J, Jiao H, Kaizerman J, et al. Potent and highly selective hypoxia-activated achiral phosphoramidate mustards as anticancer drugs. *J Med Chem.* 2008;51:2412–2420. doi:10.1021/jm701028q

19. Nepali K, Lee H, Liou J. Nitro-group-containing drugs. *J Med Chem.* 2019;62:2851–2893. doi:10.1021/acs.jmedchem.8b00147
20. Cheng W, Zhou J, Tian X, et al. Development of the third generation EGFR tyrosine kinase inhibitors for anticancer therapy. *Curr Med Chem.* 2016;23:3343–3359.
21. Wang C, Gao H, Dong J, et al. Insight into the medicinal chemistry of EGFR and HER-2 inhibitors. *Curr Med Chem.* 2014;21(11):1336–1350.
22. Ikeda Y, Hisano H, Nishikawa Y, et al. Targeting and treatment of tumor hypoxia by newly designed prodrug possessing high permeability in solid tumors. *Mol Pharm.* 2016;13(7):2283–2289. doi:10.1021/acs.molpharmaceut.6b00011
23. Wood ER, Truesdale AT, McDonald OB, et al. A unique structure for epidermal growth factor receptor bound to GW572016 (Lapatinib): relationships among protein conformation, inhibitor off-rate, and receptor activity in tumor cells. *Cancer Res.* 2004;64(18):6652–6659. doi:10.1158/0008-5472.CAN-04-1168
24. Frearson PM, Stern ES. Some new analogues of pethidine. Part III. 1-aryloxy-alkylpethidines, and close analogues. *J Chem Soc.* 1958:3065–3067.
25. Liu H, Ji M, Luo XM, et al. New p-methylsulfonamido phenylethylamine analogues as class III antiarrhythmic agents: design, synthesis, biological assay, and 3D-QSAR analysis. *J Med Chem.* 2002;45(14):2953–2969. doi:10.1021/jm010574u
26. Ple PA, Green TP, Hennequin LF, et al. Discovery of a new class of anilinoquinazoline inhibitors with high affinity and specificity for the tyrosine kinase domain of c-Src. *J Med Chem.* 2004;47(4):871–887. doi:10.1021/jm030317k
27. Marzaro G, Guiotto A, Pastorini G, et al. A novel approach to quinazolin-4(3H)-one via quinazoline oxidation: an improved synthesis of 4-anilinoquinazolines. *Tetrahedron.* 2010;66(4):962–968. doi:10.1016/j.tet.2009.11.091
28. Lueth A, Lowe W. A novel synthesis of EGFR-tyrosine-kinase inhibitors with 4-(indol-3-yl)quinazoline structure. *J Heterocyclic Chem.* 2008;45(3):703–708. doi:10.1002/jhet.5570450311
29. Zhou W, Liu XF, Tu ZC, et al. Discovery of pteridin-7(8H)-one-based irreversible inhibitors targeting the epidermal growth factor receptor (EGFR) kinase T790M/L858R mutant. *J Med Chem.* 2013;56(20):7821–7837. doi:10.1021/jm401045n

## Drug Design, Development and Therapy

Dovepress

### Publish your work in this journal

Drug Design, Development and Therapy is an international, peer-reviewed open-access journal that spans the spectrum of drug design and development through to clinical applications. Clinical outcomes, patient safety, and programs for the development and effective, safe, and sustained use of medicines are a feature of the journal, which has also

been accepted for indexing on PubMed Central. The manuscript management system is completely online and includes a very quick and fair peer-review system, which is all easy to use. Visit <http://www.dovepress.com/testimonials.php> to read real quotes from published authors.

Submit your manuscript here: <https://www.dovepress.com/drug-design-development-and-therapy-journal>